Full-Vectorial Matched Interface and Boundary (MIB) Method for the Modal Analysis of Dielectric Waveguides

Shan Zhao

***Abstract*—This paper introduces the matched interface and boundary (MIB) method for the eigenmode analysis of two dimensional step-index waveguides. The MIB method distinguishes itself from other existing interface methods by avoiding the use of the Taylor series expansion and by introducing the concept of the iterative use of low-order jump conditions. The difficulty associated with other interface approaches in extending to ultrahigh order is thus bypassed in the MIB method. In solving rectangular waveguide with a single straight interface, the MIB interface treatment can be carried out systematically so that the resulting scalar approach is of arbitrarily high order, in principle. Orders up to 12 are confirmed numerically for both transverse magnetic and transverse electric modes. In dealing with rectangular waveguide with a dielectric corner, a novel full-vectorial MIB method is proposed, in which an advanced corner handling technique is applied to accommodate the singular behavior of field near the corner. Benchmark problems are employed to validate the proposed full-vectorial approach. Higher order convergence is achieved numerically.**

***Index Terms*—Dielectric corner, dielectric interface, finite difference, high-order method, matched interface and boundary, step-index waveguide.**

I. Introduction

STEP-INDEX type optical waveguides are basic building blocks of optoelectronic devices. Numerical simulation is an indispensable tool for the test and design of such devices. Many of these optical simulations are carried out in the framework of finite-difference modeling. However, due to the field discontinuities, the numerical accuracy of the finite-difference schemes commonly deteriorates at material interfaces [1]. In order to restore the accuracy, special interface treatments are required to enforce the physical interface conditions in the finite-difference discretization.

The importance and challenge of maintaining numerical accuracy near the dielectric interface have stimulated much effort in the recent years. The first treatment of this kind was considered by Stern [2] in his pioneer semivectorial approach. By taking into account the polarization effects, this interface treatment is essentially achieved via averaging the permittivity over meshes. A more flexible approach, based on the Taylor series expansion, was proposed by Vassallo [3]. His finite-difference scheme can achieve uniformly second-order convergence for step-index waveguides. Since then, several modified finite-difference schemes/equations with second-order accuracy have been formulated [4]–[6].

It is well known that, compared with the common second-order finite difference methods, higher order schemes could not only deliver high accuracy with the use of usual grids but also allow the use of coarse grids while still maintaining good accuracy. Furthermore, as noted by Hadley [7], the very coarse grid of the higher order finite-difference schemes will lead to dramatic savings in computational effort, so that large-scale photonic problems that are previously intractable can be solved. Thus, there is much research interest in the field of step-index waveguides [1] to develop higher order finite-difference schemes. Nevertheless, when formulating higher order schemes, the proper enforcement of higher order interface conditions becomes extremely important [8]. In particular, higher order interface schemes are *indispensable* for designing new higher order finite-difference schemes that really achieve higher order convergence.

Most such higher order interface schemes in the field are constructed based on the Taylor series expansion and via the matching of higher order jump conditions across the interface. For example, up to third-order jump conditions were used in Vassallo's three-point generalized Douglas scheme with a truncation error of $O(\Delta^4)$ [1]. Similarly, higher order interface schemes using jump conditions of fourth order [9] and sixth order [10] are considered in the literature. Chiou *et al.* [11] proposed another interface scheme based on a generalized Taylor series expansion, with which up to fifth-order jump conditions can be enforced. With this new interface modeling, fourth-order accurate generalized Douglas formulas were derived for both one-dimensional [11] and two-dimensional [12] step-index waveguides. The full-vectorial interface matching involving up to fourth-order coupled jump conditions has also been proposed in a higher order finite-difference approach [13].

Also based on the Taylor expansion, the derivation of several finite-difference equations with higher order accuracy has been presented by Hadley [7], [14], [15] for photonic simulations. By properly matching zeroth- and first-order jump conditions, a quasi-fourth-order approximation is derived for (1-D) beam propagation [7]. The method has been extended to deal with (2-D) step-index waveguides with nearly 1-D structures [14]. Later, by using a similar interface treatment, but considering formal infinite series solution of the 2-D Helmholtz equation involving Bessel functions, sines, and cosines, a full-vectorial

Manuscript received December 20, 2007; revised March 17, 2008. Published August 29, 2008 (projected). This work was supported in part by National Science Foundation Grants DMS-0731503 and DMS-0616704.

The author is with the Department of Mathematics, University of Alabama, Tuscaloosa, AL 35487 USA (e-mail: szhao@bama.ua.edu).

Color versions of one or more of the figures in this paper are available online at http://ieeexplore.ieee.org.

Digital Object Identifier 10.1109/JLT.2008.923226

finite difference equation method is constructed [15], which can attain sixth-order accuracy for 2-D straight interface problems.

Another grand challenge in the design of higher order finite-difference approaches for optical simulation is due to the singular field behavior associated with a dielectric corner [16]. A thorough semianalytical derivation of finite-difference equations that satisfy correct physical conditions at a dielectric corner has been considered by Hadley [17]. This leads to a highly accurate full-vectorial modal analysis for 2-D waveguides with dielectric corners. This corner treatment has been significantly improved by Thomas *et al.* [13] in their full-vectorial finite difference method so that a third-order convergence could be secured for dielectric corner problems.

The success of all aforementioned interface schemes lies in the clever use of two major mathematical components: the Taylor expansion and high-order jump conditions. However, it is also due to such two components that the generalization of these interface schemes to even higher order is technically challenging, because it will involve formidable algebra. In this paper, we will propose a fundamentally different interface scheme, the matched interface and boundary (MIB) method, for modal analysis of rectangular dielectric waveguides. The MIB was first proposed for solving Maxwell's equations with straight interfaces [8], and it has been recently generalized to treat curved interfaces [18] and shape-edged interfaces [19] for solving the Poisson equations. The MIB has also been reformulated to impose complex boundary conditions for high-order collocation methods [20].

The MIB method distinguishes itself from other existing interface methods by avoiding the use of the Taylor expansion and by introducing the concept of the iterative use of low-order jump conditions. The difficulty associated with other interface approaches in extending to ultrahigh order is thus simply bypassed in the MIB method. Moreover, the MIB modeling is systematically carried out and can be made to arbitrarily high order in principle. For example, MIB schemes of up to twelfth order have been constructed for time-domain electromagnetic problems with straight interfaces [8]. For curved interfaces, up to sixth-order schemes have been demonstrated for elliptic interface problems [18].

The objectives of this paper are twofold. First, a scalar MIB method will be introduced for solving Helmholtz equations with single straight material interface. The new scheme restores the convergence rate of finite-difference simulations at dielectric interface to arbitrarily high orders for step-index optical waveguides. Secondly, coupled with an advanced corner treatment [13], a full-vectorial MIB approach will be introduced to deal with the rectangular-type dielectric waveguides. Higher order convergence is also achieved. The rest of this paper is organized as follows. Section II is devoted to the theory and algorithm of the scalar and full-vectorial MIB methods. Numerical tests are carried out to validate the proposed method in Section III. A conclusion ends this paper.

II. Theory and Algorithm

In this section, we introduce the matched interface and boundary methods for modal analysis of dielectric waveguides with straight interfaces and dielectric corners. To this end, scalar and full-vectorial eigenvalue problems of Helmholtz equations will be solved, respectively.

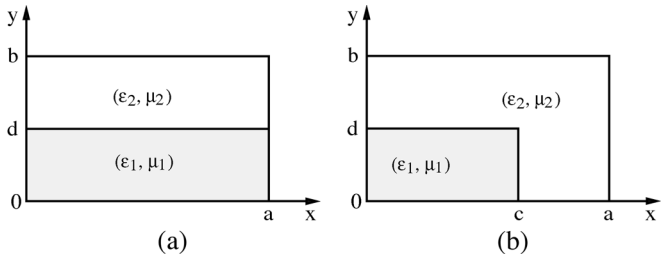

Fig. 1. Illustration of partially dielectric-filled rectangular waveguides (a) with a single dielectric interface and (b) with a dielectric corner.

A. Interface Schemes for Straight Interfaces

Consider a partially filled rectangular waveguide with a material interface perpendicular to the x- or y-axis. A typical configuration is shown in Fig. 1(a). For such a configuration, the electromagnetic field modes will be hybrid ones that are combinations of TE^y and TM^y modes [22]. Except on interfaces, it is sufficient to consider the following two scalar Helmholtz equations, respectively, for TE^y mode:

$$\frac{\partial^2 E}{\partial x^2} + \frac{\partial^2 E}{\partial y^2} + k_0^2 \epsilon E = \beta^2 E \tag{1}$$

and TM^y mode

$$\frac{\partial^2 H}{\partial x^2} + \frac{\partial^2 H}{\partial y^2} + k_0^2 \epsilon H = \beta^2 H. \tag{2}$$

Here $E = E_z$ and $H = H_z$, β is the propagation constant, ϵ is the relative permittivity coefficient, and $k_0 = 2\pi/\lambda$ is the free-space wave number with λ being the free-space wavelength.

In this paper, the MIB method will be formulated for solving TM^y mode only. The corresponding jump conditions that should be enforced to couple field solutions in both dielectric media are

$$[H] = H^+ - H^- = 0 \tag{3}$$

$$\left[\frac{1}{\epsilon}\frac{\partial H}{\partial y}\right] = \frac{1}{\epsilon^+}\frac{\partial H^+}{\partial y} - \frac{1}{\epsilon^-}\frac{\partial H^-}{\partial y} = 0 \tag{4}$$

where the superscript $-$ or $+$ denotes the limiting value of a function from, respectively, the negative or positive side of the interface $y = d$. Thus, $\epsilon^+ = \epsilon_2$ and $\epsilon^- = \epsilon_1$ in Fig. 1(a). The zeroth- and first-order jump conditions (3) and (4) will be iteratively imposed to construct higher order interface treatments in the MIB method, so that the use of higher order jump conditions, which is numerically too involved [8], is simply avoided. The MIB solution of TE^y mode can be similarly constructed by considering the corresponding jump conditions

$$[E] = 0, \quad \left[\frac{\partial E}{\partial y}\right] = 0. \tag{5}$$

In this paper, a uniform grid is assumed for simplicity. It is noted that the interface $y = d$ may not need to be laid on the grid in the present modeling. In the MIB methods [8], [18], [19], the standard $(2M)$th-order central finite-difference approximation

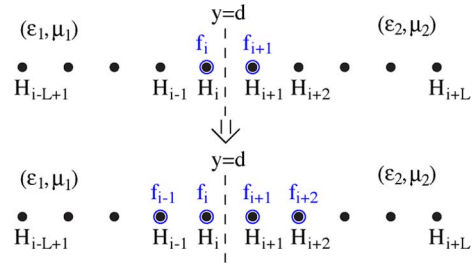

Fig. 2. Illustration of fictitious and original grid points used in the MIB scheme. The fictitious points are shown as open circles, while the original grid points are shown as filled circles.

[20] will be carried out away from the interface, while the finite-difference weights of nodes in the vicinity of the interface, i.e., the so-called irregular points, shall be modified in order to satisfy jump conditions. A universal rule here is that, to approximate function or its derivatives on one side of interface, one never *directly* refers to function values from the other side. Instead, in the MIB scheme, fictitious values from the other side of the interface will be used. For example, consider a uniform grid $(y_1, y_2, \ldots, y_N)$, with $y_i < d < y_{i+1}$. Denote the function value and fictitious value at the node y_i as H_i and f_i, respectively. See Fig. 2. The second-order finite-difference approximations near the interface will be modified to be

$$\frac{\partial^2 H(y_i)}{\partial y^2} = \frac{H_{i-1} - 2H_i + f_{i+1}}{\Delta y^2}$$
$$\frac{\partial^2 H(y_{i+1})}{\partial y^2} = \frac{f_i - 2H_{i+1} + H_{i+2}}{\Delta y^2}. \tag{6}$$

The general $(2M)$th-order central finite-difference approximations can be similarly modified, which calls for a total of $2M$ fictitious points on both sides of the interface. These fictitious values will be resolved based on the discretized jump conditions.

Referring to Fig. 2, at the first step, we determine two fictitious values f_i and f_{i+1} by discretizing two jump conditions (3) and (4) in the same manner of (6), i.e., never referring to function values across the interface

$$\sum_{k=1}^{L} w^{-}_{0,k} H_{i-L+k} + w^{-}_{0,L+1} f_{i+1} = w^{+}_{0,1} f_i + \sum_{k=2}^{L+1} w^{+}_{0,k} H_{i+k-1} \tag{7}$$

$$\frac{1}{\epsilon^-}\left(\sum_{k=1}^{L} w^{-}_{1,k} H_{i-L+k} + w^{-}_{1,L+1} f_{i+1}\right) = \frac{1}{\epsilon^+}\left(w^{+}_{1,1} f_i + \sum_{k=2}^{L+1} w^{+}_{1,k} H_{i+k-1}\right) \tag{8}$$

where $w^{-}_{j,k}$ and $w^{+}_{j,k}$ for $k = 1, \ldots, L+1$ and $j = 0, 1$ are one-sided finite difference weights, respectively, for left and right subdomains. Here the subscript j represents interpolation ($j = 0$) and the first-order derivative approximation ($j = 1$), and k is for grid index. These finite-difference weights can be generated through a call to a small subroutine presented in [21]. One-sided approximations involving L grid nodes in one side are used to ensure the sufficiently high accuracy. By solving (7) and (8), one can determine fictitious values f_i and f_{i+1}. We note that the solved fictitious value is actually a linear combination that represents f_i or f_{i+1} in terms of corresponding function values $(H_{i-L+1}, \ldots, H_{i+L})$ [8], [20]. By substituting f_i and f_{i+1} into (6), a second-order MIB method can be constructed.

To achieve the fourth-order accuracy, we determine two more fictitious values by enforcing two jump conditions (3) and (4) again

$$\sum_{k=1}^{L} \tilde{w}^{-}_{0,k} H_{i-L+k} + \tilde{w}^{-}_{0,L+1} f_{i+1} + \tilde{w}^{-}_{0,L+2} f_{i+2} = \tilde{w}^{+}_{0,1} f_{i-1} + \tilde{w}^{+}_{0,2} f_i + \sum_{k=3}^{L+2} \tilde{w}^{+}_{0,k} H_{i+k-2}$$

$$\frac{1}{\epsilon^-}\left(\sum_{k=1}^{L} \tilde{w}^{-}_{1,k} H_{i-L+k} + \tilde{w}^{-}_{1,L+1} f_{i+1} + \tilde{w}^{-}_{1,L+2} f_{i+2}\right) = \frac{1}{\epsilon^+}\left(\tilde{w}^{+}_{1,1} f_{i-1} + \tilde{w}^{+}_{1,2} f_i + \sum_{k=3}^{L+2} \tilde{w}^{+}_{1,k} H_{i+k-2}\right)$$

where the finite-difference weights $\tilde{w}^{-}_{j,k}$ and $\tilde{w}^{+}_{j,k}$ are different from those in (7) and (8) because they involve a different set of grid points; see Fig. 2. From these two equations, two new unknowns f_{i-1} and f_{i+2} can be determined, since f_i and f_{i+1} are known. With these four fictitious values, standard fourth-order central finite-difference approximations can be evaluated at either y_i or y_{i+1}, in a manner similar to (6). This gives rise to a fourth-order MIB method.

By iteratively determining two more fictitious points at each step, finally we can attain $2M$ fictitious points for a $(2M)$th-order central finite-difference approximation across the interface. For the present rectangular waveguides with a single interface, such a procedure can be carried out systematically and is thus of arbitrarily high order in principle. Numerically, the order of accuracy of the MIB method might be limited by the parameter L. To ensure the stability, in practice, $L > 14$ is hardly used [20]. Nevertheless, by using a large enough L, up to twelfth order of convergence has been verified in the literature [8], which is still considerably superior than any other interface schemes reported in the literature. Moreover, MIB schemes with $M > L$ can be generated via more iterations [20]. Finally, we note that the MIB interface matching need only be carried out once along one y grid line. The solved representation coefficients can then be used in any other y grid lines [8], [20].

We note that the matrix bandwidth of the proposed approach is determined by M at regular grid points. At irregular points, such a bandwidth will be further extended if $L > M$. Consequently, for a twelfth-order MIB scheme, the bandwidth will be much larger than that of the lower order finite-difference schemes. Nevertheless, such a MIB scheme is actually cost-effective because a coarse mesh will be sufficient to achieve a good accuracy [8].

B. Interface Schemes for Dielectric Corners

Consider a partially filled rectangular waveguide with a dielectric corner. A typical configuration is shown in Fig. 1(b).

For dielectric corner problems, it is known that field components are singular near the corner [16]. Since the transverse electric field itself diverges at the corner, transverse magnetic field components H_x and H_y are conventionally used for modal analysis [13], [17]. Both H_x and H_y satisfy the scalar Helmholtz equation (2) away from the interfaces. However, on the interfaces, the jump conditions couple H_x and H_y together so that a full-vectorial finite difference approach is necessary for rectangular waveguides with dielectric corners. Moreover, to achieve high-order convergence, an appropriate corner treatment to account for the field singularity is indispensable [13], [17].

We first derive jump conditions. Across the interfaces, we have that both H_x and H_y are continuous

$$[H_x] = 0, \quad [H_y] = 0. \tag{9}$$

By using the divergence-free property, one has the continuity of the normal derivative of the normal component of $\mathbf{H}$

$$\left[\frac{\partial H_n}{\partial n}\right] = 0 \tag{10}$$

where n denotes the normal direction. Finally, the continuity of E_z gives rise to

$$\left[\frac{1}{\epsilon}\frac{\partial H_x}{\partial y}\right] = \left[\frac{1}{\epsilon}\frac{\partial H_y}{\partial x}\right]. \tag{11}$$

These zeroth- and first-order jump conditions were used in the interface schemes reported in [13] and [17]. However, unlike the interface scheme considered in [13], higher order jump conditions will not be used in the proposed MIB method.

Consider the configuration shown in Fig. 1(b). Away from the corner and interfaces, standard central finite-difference approximations of the Helmholtz equations for both H_x and H_y are carried out. Away from the corner, the MIB interface treatments for both H_x and H_y will be similarly conducted as in Section II-A. For simplicity, we will discuss in detail the MIB scheme across the interface with $x = c$ and $y < d$, and the MIB scheme for the other interface can be similarly formulated. Along the interface $x = c$ and $y < d$, jump conditions for H_x are

$$[H_x] = 0, \quad \left[\frac{\partial H_x}{\partial x}\right] = 0. \tag{12}$$

These two conditions will be iteratively enforced to generate $2M$ fictitious values for H_x on both sides of the interface, so that the general $(2M)$th-order central finite differences can be applied. The MIB scheme for H_y calls for additional numerical treatments, since the jump conditions for H_y now involve H_x

$$[H_y] = 0, \quad \left[\frac{1}{\epsilon}\frac{\partial H_y}{\partial x}\right] = \left[\frac{1}{\epsilon}\frac{\partial H_x}{\partial y}\right] = \left(\frac{1}{\epsilon^+} - \frac{1}{\epsilon^-}\right)\frac{\partial H_x}{\partial y}. \tag{13}$$

It is noted that the right-hand side of the first-order jump condition has been simplified because the tangential derivative of normal component H_x is continuous, i.e., $\partial H_x/\partial y = \partial H_x^+/\partial y = \partial H_x^-/\partial y$. The nonhomogeneous term in (13) will be treated in essentially two steps. First, the general MIB interface treatments for jump conditions involving source terms will be conducted. Secondly, $\partial H_x/\partial y$ will be accurately calculated via standard high-order finite differences and interpolations.

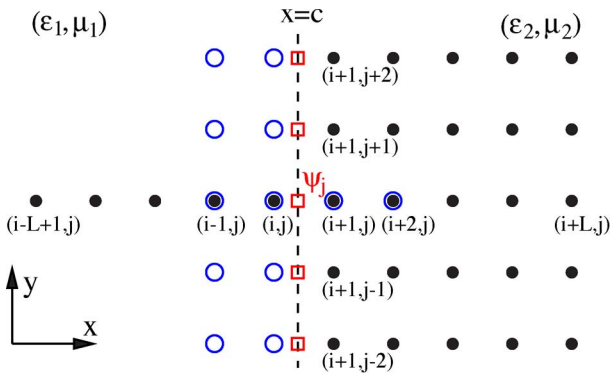

Fig. 3. An illustration of interface treatment of the full-vectorial MIB method. The fictitious points and original grid points are shown as, respectively, open circles and filled circles. Here ψ_j will be first approximated along the interface (dashed line) in terms of auxiliary points (open squares), then will be interpolated along x direction.

Referring to Fig. 3, we denote the function value and fictitious value of H_y at the node (x_i, y_j) as H_i and f_i, respectively, and let $\psi_j = (\partial/\partial y)H_x(c, y_j)$. Jump conditions (13) will be discretized as

$$\sum_{k=1}^{L} w_{0,k}^{-} H_{i-L+k} + w_{0,L+1}^{-} f_{i+1} = w_{0,1}^{+} f_i + \sum_{k=2}^{L+1} w_{0,k}^{+} H_{i+k-1} \tag{14}$$

$$\frac{1}{\epsilon^-}\left(\sum_{k=1}^{L} w_{1,k}^{-} H_{i-L+k} + w_{1,L+1}^{-} f_{i+1}\right) = \frac{1}{\epsilon^+}\left(w_{1,1}^{+} f_i + \sum_{k=2}^{L+1} w_{1,k}^{+} H_{i+k-1}\right) + \frac{(\epsilon^+ - \epsilon^-)\psi_j}{\epsilon^- \epsilon^+} \tag{15}$$

from which f_i and f_{i+1} can be solved as linear combinations in terms of $(H_{i-L+1}, \ldots, H_{i+L}, \psi_j)$. Similarly, other fictitious values are also solved as linear combinations in terms of $(H_{i-L+1}, \ldots, H_{i+L}, \psi_j)$ after iterative matching. Like in the previous cases, such a MIB representation needs to be carried out only once. Then it can be used for different y grid lines, albeit ψ_j should be estimated for a different j.

To estimate $\psi_j = (\partial/\partial y)H_x(c, y_j)$, an appropriate central finite difference will be used to approximate the y derivative along the interface; see Fig. 3. The order of such an approximation shall be at least the same as the overall MIB modeling. For example, a fourth MIB treatment is illustrated in Fig. 3, which involves four auxiliary points on the interface

$$\psi_j = \frac{\partial H_x(c, y_j)}{\partial y} = \frac{1}{\Delta y}\left(\frac{1}{12}H_x(c, y_{j-2}) - \frac{2}{3}H_x(c, y_{j-1}) + \frac{2}{3}H_x(c, y_{j+1}) - \frac{1}{12}H_x(c, y_{j+2})\right). \tag{16}$$

These auxiliary points will then be interpolated along each x grid line by using grid nodes and fictitious points exclusively from one side of the interface. We note that in such a procedure, one has certain flexibility in choosing auxiliary points and grid nodes to interpolate them, as long as the requirement of order of accuracy is satisfied. In Fig. 3, these auxiliary points are interpolated using L grid nodes from the right and two fictitious points from the left for which fourth-order MIB representations in terms of H_x values are available in the previous calculations.

Like in previous studies, all finite-difference approximation kernels and interpolation kernels involved in this paper are generated automatically via a call to the subroutine presented in [21]. Therefore, this MIB interface treatment can still be carried out systematically, and is thus of arbitrarily high order in principle. Numerically, the order of the proposed MIB method will be controlled via a user-input parameter M, which determines the order of all finite differences and interpolations being used.

C. Corner Treatments

By appropriately choosing mesh size so that the corner point is not located on grid, it seems that the additional corner treatment might be avoided because the jump conditions considered in the last section are in fact valid for all irregular points of both perpendicular interfaces. The aforementioned MIB schemes can thus be applied, except that one-sided finite differences should be used for estimating ψ_j near the corner. However, such a discretization has been numerically found to be at most of second-order accuracy. In fact, this order reduction has been pointed out by many authors [13], [16], [17] and is due to the singular behavior of field components in the vicinity of the corner. In particular, it has been noted [13], [17] that all corner treatments based on Taylor series methods, which include the current attempt because the finite differences are derived from the Taylor expansion, are doomed to be inaccurate. Instead, different local expansions were suggested, from which semianalytical corner treatments were constructed [13], [17].

In the following study, the state-of-art corner treatment introduced in [13] will be used for the $2M \times 2M$ grid points surrounding the corner. Consider a local coordinate as shown in Fig. 4(a). H_x and H_y will be approximated in the vicinity of the corner as

$$H_x(r,\theta) = \sum_{k=1}^{12} c_k u_k^x(r,\theta), \quad H_y(r,\theta) = \sum_{k=1}^{12} c_k u_k^y(r,\theta) \tag{17}$$

where c_k are undetermined coefficients $u_k^x = u_k^{x'} - u_k^{y'}$ and $u_k^y = u_k^{x'} + u_k^{y'}$, while the explicit expressions for $u_k^{x'}$ and $u_k^{y'}$ can be found in [13]. To derive a difference equation for a node (x_i, y_j) near the corner, one needs to first determine 12 unknown coefficients involved in (17). This can be achieved by fitting (17) to H_x and H_y values on six grid nodes. In other words, $(c_1, c_2, \ldots, c_{12})$ are representation coefficients that express $H_x(x_i, y_j)$ and $H_y(x_i, y_j)$ in terms of six surrounding nodes. After solving $(c_1, c_2, \ldots, c_{12})$, termwise differentiations are given in [13] so that the discretization of the Helmholtz equation can be simply formed. Here, we note the flexibility in choosing the stencil surrounding (i, j). In this paper, we first fix five nodes as in the regular five-point finite difference, i.e., $(i-1, j)$, (i, j), $(i+1, j)$, $(i, j-1)$, and $(i, j+1)$. The sixth node will be chosen depending on the media. For the corner configuration shown in Fig. 4(b), we will pick up $(i-1, j-1)$ if $\epsilon_1 < \epsilon_2$, and $(i+1, j+1)$ otherwise. The convergence rate of such a stencil selection has been numerically found to be slightly more uniform. After selection, the same stencil will be used for all irregular points near the corner.

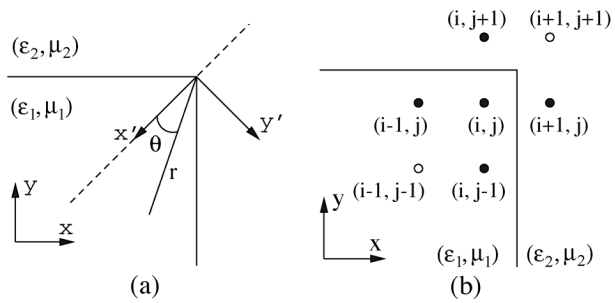

Fig. 4. (a) Local coordinate system used in the corner treatment. (b) Stencil used in the corner treatment. If $\epsilon_1 > \epsilon_2$, $(i-1, j-1)$ will be used. Otherwise, $(i+1, j+1)$ will be used. The same stencil will be used for all irregular points near the corner.

The order of accuracy of this corner treatment is known to be third order [13]. Consequently, the overall order of the proposed full-vectorial MIB approach is also limited to third order, even though away from corner, ultrahigh orders can still be achieved in the MIB interface treatments. The extension of the current full-vectorial approach to high order is possible, provided a higher order corner treatment is utilized.

III. Numerical Experiments

This section is devoted to the numerical tests of the proposed MIB method for rectangular waveguides with a single interface and two perpendicular interfaces. In all numerical studies, only the fundamental mode is computed and reported through the use of an iterative eigenvalue solver [23]. Other standard eigenvalue solvers have also been tested, which yield the same results.

A. Numerical Results for Straight Interfaces

We first validate the proposed MIB method by considering a partially filled waveguide with a single straight interface; see Fig. 1(a). By assuming the perfect electric conducting (PEC) conditions in all boundaries for both E_z and H_z, the analytical solutions of both TE^y and TM^y modes are available [22]. The detailed analytical expressions are given in Appendix A. In this paper, the model parameters are chosen as follows: $a = 2.25$, $b = 1$, $d = 0.5$, $\lambda = 1.55$, $\epsilon_1 = 8$, and $\epsilon_2 = 1$. By using a computer algebra system, such as *Maple,* the effective propagation constant $\beta_e = \beta/k$ can be calculated to be 2.4896986225840504 and 2.7253537501434527, respectively, for TE^y and TM^y mode.

To discretize the problem, a uniform mesh with size (N_x, N_y) is used. The length of central finite-difference kernels used in x and y directions is chosen as, respectively, $2M_x+1$ and $2M_y+1$. At the PEC boundaries, the so-called antisymmetric and symmetric boundary extension [8], [20] is used, respectively, for E_z and H_z in TE^y and TM^y mode. In this paper, a sufficiently accurate discretization is used in the x direction with fixed $N_x = 21$

TABLE I
NUMERICAL CONVERGENCE TESTS OF THE SCALAR MIB SCHEMES FOR A PARTIALLY FILLED WAVEGUIDE WITH HIGH CONTRAST PROFILE. HERE $1.57(-3)$ DENOTES 1.57×10^{-3}

		TE^y			TM^y		
(M_y, L)	N_y	26	52	104	26	52	104
$(1,3)$	Error	$1.57(-3)$	$3.92(-4)$	$9.85(-5)$	$1.58(-4)$	$3.87(-5)$	$9.63(-6)$
	Order		2.00	1.99		2.03	2.01
$(2,4)$	Error	$5.32(-5)$	$3.79(-6)$	$2.54(-7)$	$4.39(-6)$	$3.18(-7)$	$2.15(-8)$
	Order		3.81	3.90		3.79	3.89
$(4,9)$	Error	$1.05(-7)$	$3.34(-10)$	$8.04(-13)$	$1.22(-8)$	$4.07(-11)$	$2.39(-13)$
	Order		8.29	8.70		8.23	7.41
$(6,13)$	Error	$8.32(-10)$	$2.18(-13)$	$2.04(-12)$	$1.31(-10)$	$1.58(-13)$	$2.39(-13)$
	Order		11.90	-3.22		6.72	-0.60

TABLE II
NUMERICAL CONVERGENCE TESTS OF THE SCALAR MIB SCHEMES FOR A PARTIALLY FILLED WAVEGUIDE WITH LOW CONTRAST PROFILE

		TE^y			TM^y		
(M_y, L)	N_y	26	52	104	26	52	104
$(1,3)$	Error	$9.63(-4)$	$2.39(-4)$	$5.93(-5)$	$1.79(-4)$	$4.40(-5)$	$1.09(-5)$
	Order		2.01	2.01		2.03	2.01
$(2,4)$	Error	$1.69(-6)$	$1.67(-7)$	$1.19(-8)$	$1.29(-6)$	$8.38(-8)$	$5.33(-9)$
	Order		3.34	3.81		3.95	3.97
$(4,9)$	Error	$1.03(-9)$	$1.59(-12)$	$3.11(-14)$	$9.64(-11)$	$1.40(-13)$	$6.94(-13)$
	Order		9.33	5.68		9.43	-2.31
$(6,13)$	Error	$1.08(-12)$	$2.47(-12)$	$6.27(-12)$	$1.30(-12)$	$1.20(-12)$	$1.13(-12)$
	Order		-1.19	-1.35		0.11	0.09

and $M_x = 16$. This spatial discretization has been numerically found to be fine enough so that the approximation errors in x direction are negligible. In y direction, across the material interface $y = d$, the MIB interface matching is carried out locally.

The absolute errors in estimating the effective eigenvalue β_e for both TE^y and TM^y modes are summarized in Table I. Scalar MIB schemes with different order, i.e., different M_y, are considered. The MIB parameter L is chosen according to M_y and is given in Table I as well. For each MIB scheme, several different mesh sizes are tested, i.e., $N_y = 26, 52$, and 104. When we double the mesh size N_y, the numerical convergence order can be simply calculated as

$$\text{order} = \log_2 \left(\frac{e_{N_y}}{e_{2N_y}} \right)$$

where e_{N_y} and e_{2N_y} are the absolute error by using mesh size N_y and $2N_y$, respectively. These numerically tested orders of accuracy are also shown in Table I.

It is clear from Table I that for both TE^y and TM^y modes, the proposed MIB schemes achieve the theoretical rate of convergence, i.e., $(2M_y)$th-order for the MIB scheme with a given M_y, except when a certain precision limit of the underlying eigenvalue solver is reached. In particular, such orders are attained for $M_y = 1, 2$, and 4 for TE^y mode. For $M_y = 6$, the twelfth order is also detected numerically for TE^y mode when $N_y = 52$. Since the accuracy level is already close to the precision limitation, further refinement with $N_y = 104$ could not be able to further reduce the error. The similar convergence pattern is also observed for TM^y mode, except now the numerical errors are about one magnitude smaller. Consequently, for $M_y = 6$ and $N_y = 52$, the numerical order is just about 6.72. At last, we note that if a larger M_y is used, the MIB scheme should theoretically attain a higher order of convergence. Nevertheless, the true orders for $M_y \geq 8$ cannot be revealed numerically because the precision limit of the eigenvalue solver is already achieved by using a small N_y, e.g., $N_y = 26$. Thus, such results are not reported.

We next consider the same waveguide but with a low contrast profile, i.e., $\epsilon_1 = 2.56$ and $\epsilon_2 = 1$. The analytical effective eigenvalue β_e is known to be 1.1353451805555585 and 1.4596192660959783, respectively, for TE^y and TM^y mode. The MIB results are listed in Table II. A similar convergence pattern is observed in Table II, in comparison with Table I. However, the MIB errors now are all smaller than the corresponding ones in Table I so that the twelfth order of $M_y = 6$ could not be numerically revealed.

B. Numerical Results for Dielectric Corners

We next explore the use of the proposed full-vectorial MIB methods for rectangular waveguide with a dielectric corner. Two

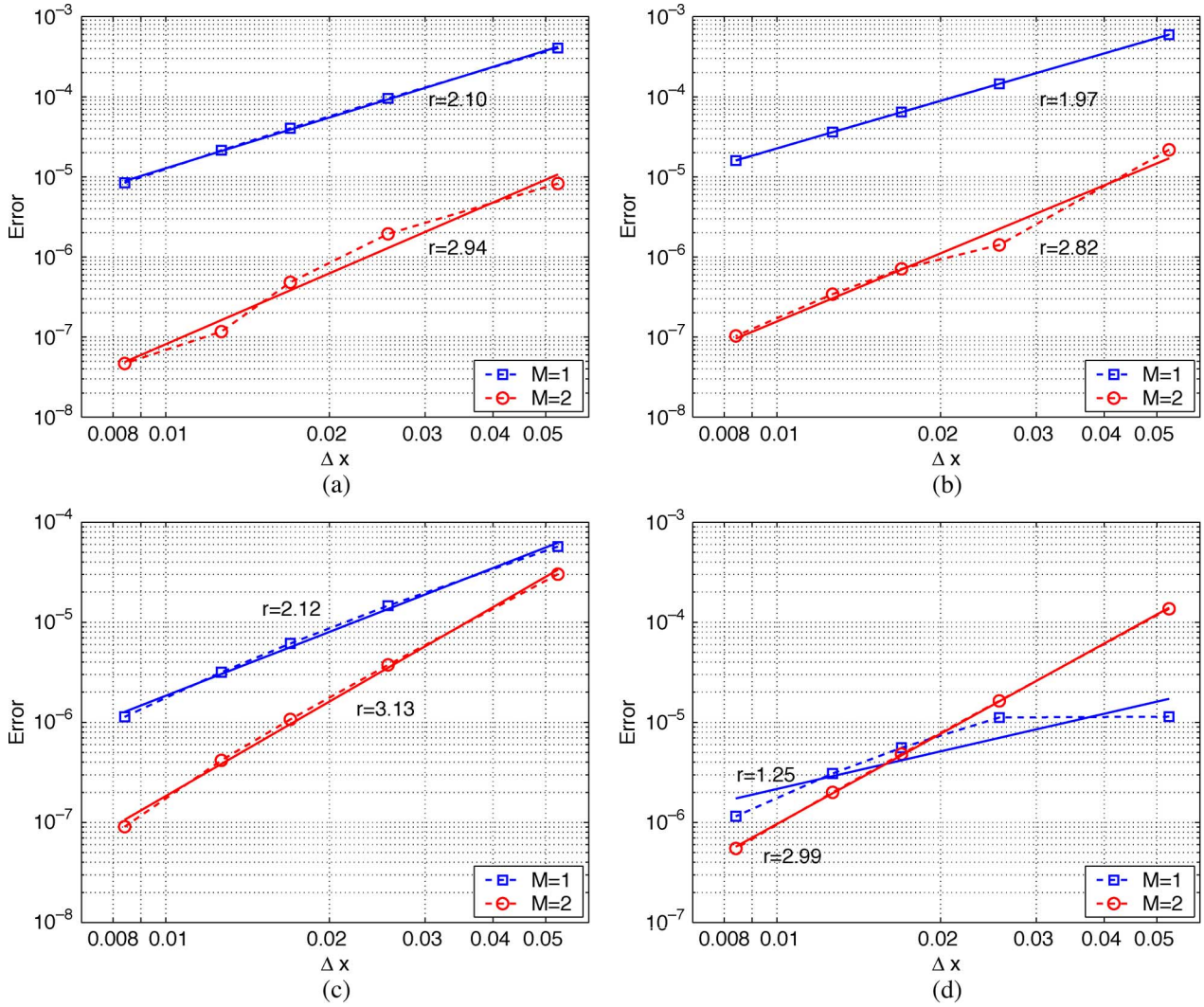

Fig. 5. Numerical convergence tests of the full-vectorial MIB schemes. (a) Case I with low contrast profile, (b) Case I with high contrast profile, (c) Case II with low contrast profile, and (d) Case II with high contrast profile.

benchmark tests considered in [13] and [17] will be examined. Referring to Fig. 1(b), the following model parameters are employed in both cases: $a = b = 1.0$, $c = d = 0.5$, and $\lambda = 1.5$. In Case I, for all boundaries, homogeneous Dirichlet and homogeneous Neumann conditions are used for H_x and H_y, respectively. Both low contrast profile ($\epsilon_1 = 2.25$ and $\epsilon_2 = 1$) and high contrast profile ($\epsilon_1 = 8$ and $\epsilon_2 = 1$) will be studied. In Case II, for H_y, homogeneous Neumann condition is used for upper and right boundaries and homogeneous Dirichlet condition is used for the other two boundaries. Boundary conditions for H_x are the opposite. Both low contrast profile ($\epsilon_1 = 1$ and $\epsilon_2 = 2.25$) and high contrast profile ($\epsilon_1 = 1$ and $\epsilon_2 = 8$) will be considered. For both cases, the exact propagation constants, which are accurate to eight or more decimal places, are available in [17] to benchmark numerical results. The absolute errors of the MIB schemes will be reported.

In this paper, a uniform mesh with $\Delta x = \Delta y$ or $N = N_x = N_y$ is used. In order to apply the corner treatment introduced in [13], N is chosen as the interface lying midway between adjacent grid nodes. The same bandwidth is used for finite-difference approximation in both x and y directions, i.e., $M = M_x = M_y$. As in the previous study, homogeneous Dirichlet and homogeneous Neumann conditions are imposed, respectively, via the antisymmetric and symmetric boundary extensions [8], [20].

The numerical convergence orders of the full-vectorial MIB schemes are depicted in Fig. 5. In all charts, the MIB errors with $(M, L) = (1, 3)$ and $(M, L) = (2, 5)$ are shown as dashed lines. For each MIB scheme, the numerical errors have been fitted to a straight line in the log-log scale by using the least squares (LS). In particular, the absolute error e_N is assumed to be a function of Δx with the form

$$e_N = C(\Delta x)^r = C\left(\frac{1}{N-1}\right)^r$$

where r and C are undetermined convergence coefficients. For each MIB scheme, these two coefficients can be estimated in the log-log scale by first conducting logarithms and then applying LS linear fitting. This gives rise to a solid convergence line in Fig. 5, and the corresponding slope which is actually LS-estimated numerical convergence ratio r is also given in Fig. 5.

It is clear from Fig. 5 that, for $M = 1$, the MIB scheme attains second-order convergence, except in the last test, where certain overperformance is encountered for coarse meshes. By using $M = 2$, the LS-fitted slopes are all around 3.0. This indicates that the third-order convergence is achieved numerically. In other words, the overall numerical order is dominated by the order of the corner treatment, as discussed in Section II-C. Similarly, a larger M is not able to produce a higher order convergence. Thus, unlike the previous numerical studies, MIB schemes with $M > 2$ are not considered. We finally note that the present MIB results for $M = 2$ are in good agreement with the literature results [13] in terms of convergence rates. Moreover, if relative errors were considered in Fig. 5, the MIB errors could be almost of the same magnitude as those reported in [13].

IV. Concluding Remarks

In this paper, we introduce a highly accurate interface scheme, the matched interface and boundary method for eigenmode analysis of rectangular dielectric waveguides. The MIB technique, originally proposed in [8], is the first method that provides a systematic approach to generate finite-difference schemes to arbitrarily high orders for interface problems in computational electromagnetics. Like existing higher order interface schemes, this is achieved by appropriately enforcing the physical jump conditions at material interfaces. However, fundamentally different procedures are employed in the MIB jump condition enforcement, so that the difficulties associated with other interface schemes in extending to arbitrarily high order are simply bypassed. In particular, there are two major differences. First, the MIB method introduces the concept of the iterative use of low-order jump conditions so that treatments of higher order jump conditions that can be numerically involving [8] are avoided. Secondly, the MIB is not based on the Taylor expansion. Instead, tensor product finite-difference approximation and interpolation are utilized [8]. Theoretically, we know that the finite-difference weights are derived based on the Taylor expansion. However, by using a small subroutine [21], one can numerically generate any finite-difference weights. This essentially avoids the formidable algebra involved in the manual derivation based on the Taylor expansions. Both differences are attributed to the success of the MIB method in achieving arbitrarily high order in dealing with straight interfaces and boundaries [8], [20] and to attain up to sixth order of convergence for curved interfaces and boundaries [18], [19].

In this paper, a scalar MIB method is introduced for modal analysis of rectangular waveguide with single straight interface. Both TM and TE modes are studied. Orders up to 12 are confirmed in the eigenmode analysis of partially filled waveguides. In order to enforce jump conditions of dielectric waveguide with two perpendicular interfaces, in which two Cartesian components of the magnetic field are coupled, a novel full-vectorial MIB method is proposed. Moreover, to account for the singular behavior of the field in the vicinity of the dielectric corner, a superior corner-handling technique [13] is utilized in the present full-vectorial MIB approach. Benchmark problems are employed to validate the proposed full-vectorial approach. Higher order of convergence is attained numerically. The generalization of the full-vectorial MIB method to deal with curved interfaces is currently under the consideration.

Appendix A
Analytical Solutions

For the TE^y mode with PEC boundaries, the eigenvector solution of (1) can be given as [22]

$$E_z = \begin{cases} A_1 \sin\left(\frac{n\pi}{a}x\right)\sin(hy)e^{-j\beta z}, & 0 \le y \le d \\ A_2 \sin\left(\frac{n\pi}{a}x\right)\sin\left(p(b-y)\right)e^{-j\beta z}, & d \le y \le b \end{cases} \tag{18}$$

where n is an integer, $n = 1, 2, 3, \ldots$, and p and h can be obtained via

$$k_0^2(\epsilon_1 - \epsilon_2) + p^2 = h^2 \tag{19}$$

$$p\cot\left(p(b-d)\right) = -h\cot(hd). \tag{20}$$

Solving p and h from (19) and (20) and taking $n = 1$, the propagation constant β is given as

$$\beta = \sqrt{k_0^2\epsilon_1 - h^2 - \left(\frac{n\pi}{a}\right)^2} = \sqrt{k_0^2\epsilon_2 - p^2 - \left(\frac{n\pi}{a}\right)^2}. \tag{21}$$

Similarly, for the TM^y mode with PEC boundaries, the eigenvector solution of (2) is

$$H_z = \begin{cases} A_1 \cos\left(\frac{n\pi}{a}x\right)\cos(hy)e^{-j\beta z}, & 0 \le y \le d \\ A_2 \cos\left(\frac{n\pi}{a}x\right)\cos\left(p(b-y)\right)e^{-j\beta z}, & d \le y \le b \end{cases} \tag{22}$$

where p and h satisfy (19) and

$$\frac{p}{\epsilon_2}\tan\left(p(b-d)\right) = -\frac{h}{\epsilon_1}\tan(hd). \tag{23}$$

Solving p and h from (19) and (23) and taking $n = 0$, the propagation constant β is also given by (21). For both TE^y and TM^y modes, the effective propagation constant $\beta_e = \beta/k_0$ will be reported.

References

[1] C. Vassallo, "Interest of improved three-point formulas for finite-difference modeling of optical devices," *J. Opt. Soc. Amer. A*, vol. 14-12, pp. 3273–3284, 1997.

[2] M. S. Stern, "Semivectorial polarised finite difference method for optical waveguides with arbitrarily index profiles," *Proc. Inst. Elect. Eng. Optoelectron.*, vol. 135, pt. J, pp. 56–63, 1988.

[3] C. Vassallo, "Improvement of finite difference methods for step-index optical waveguides," *Proc. Inst. Elect. Eng. Optoelectron.*, vol. 139, pt. J, pp. 137–142, 1992.

[4] P. Lüsse, P. Stuwe, J. Schüle, and H.-G. Unger, "Analysis of vectorial mode fields in optical waveguides by a new finite difference method," *J. Lightw. Technol.*, vol. 12, pp. 487–494, 1994.

[5] G. R. Hadley and R. E. Smith, "Full-vector waveguide modeling using an iterative finite-difference method with transparent boundary conditions," *J. Lightw. Technol.*, vol. 13, pp. 465–469, 1995.

[6] J. S. Xia and J. Z. Yu, "New finite-difference scheme for simulations of step-index waveguides with tilt interfaces," *IEEE Photon. Technol. Lett.*, vol. 15, pp. 1237–1239, 2003.

[7] G. R. Hadley, "Low-truncation-error finite difference equations for photonics simulation I: Beam propagation," *J. Lightw. Technol.*, vol. 16-1, pp. 134–141, 1998.

[8] S. Zhao and G. W. Wei, "High-order FDTD methods via derivative matching for Maxwell's equations with material interfaces," *J. Comput. Phys.*, vol. 200, pp. 60–103, 2004.

[9] R. Stoffer and H. J. W. M. Hoekstra, "Efficient interface conditions based on a 5-point finite difference operator," *Opt. Quantum Electron.*, vol. 30, pp. 375–383, 1998.

[10] H. A. Jamid and M. N. Akram, "A new higher order finite-difference approximation scheme for the method of lines," *J. Lightw. Technol.*, vol. 19, pp. 398–404, 2001.
[11] Y. P. Chiou, Y. C. Chiang, and H. C. Chang, "Improved three-point formulas considering the interface conditions in the finite-difference analysis of step-index optical devices," *J. Lightw. Technol.*, vol. 18, pp. 243–251, 2000.
[12] J. Yamauchi, T. Murata, and H. Nakano, "Semivectorial H-field analysis of rib waveguides by a modified beam-propagation method based on the generalized Douglas scheme," *Opt. Lett.*, vol. 25-24, pp. 1171–1173, 2000.
[13] N. Thomas, P. Sewell, and T. M. Benson, "A new full-vectorial higher order finite-difference scheme for the modal analysis of rectangular dielectric waveguides," *J. Lightw. Technol.*, vol. 25, pp. 2563–2570, 2007.
[14] G. R. Hadley, "Low-truncation-error finite difference equations for photonics simulation II: Vertical-cavity surface-emitting lasers," *J. Lightw. Technol.*, vol. 16-1, pp. 142–151, 1998.
[15] G. R. Hadley, "High-accuracy finite-difference equations for dielectric waveguide analysis I: Uniform regions and dielectric interfaces," *J. Lightw. Technol.*, vol. 20, pp. 1210–1218, 2002.
[16] A. S. Sudbo, "Why are accurate computations of mode fields in rectangular dielectric waveguides difficult?," *J. Lightw. Technol.*, vol. 10, pp. 418–419, 1992.
[17] G. R. Hadley, "High-accuracy finite-difference equations for dielectric waveguide analysis II: Dielectric corners," *J. Lightw. Technol.*, vol. 20, pp. 1219–1231, 2002.
[18] Y. C. Zhou, S. Zhao, M. Feig, and G. W. Wei, "High order matched interface and boundary (MIB) schemes for elliptic equations with discontinuous coefficients and singular sources," *J. Comput. Phys.*, vol. 213, pp. 1–30, 2006.
[19] S. N. Yu, Y. C. Zhou, and G. W. Wei, "Matched interface and boundary (MIB) method for elliptic problems with sharp-edged interfaces," *J. Comput. Phys.*, vol. 224, pp. 729–756, 2007.
[20] S. Zhao, "On the spurious solutions in the high-order finite difference methods," *Comput. Methods Appl. Mech. Eng.*, vol. 196, pp. 5031–5046, 2007.
[21] B. Fornberg, "Calculation of weights in finite difference formulas," *SIAM Rev.*, vol. 40, pp. 685–691, 1998.
[22] C. A. Balanis, *Advanced Engineering Electromagnetics*. New York: Wiley, 1989.
[23] W. J. Stewart and A. Jennings, "A simultaneous iteration algorithm for real matrices," *ACM Trans. Math. Software*, vol. 7, pp. 184–198, 1981.

Shan Zhao was born in Guiyang, China, in 1974. He received the B.Sc. degree in mathematics from Lanzhou University, Lanzhou, China, in 1997 and the Ph.D. degree in scientific computing from National University of Singapore, in 2003.

From 2003 to 2006, he was a Postdoctoral Fellow with Michigan State University, East Lansing. In 2006, he joined the Faculty of the Mathematics Department, University of Alabama, Tuscaloosa, as an Assistant Professor. His current research interests include high-order interface schemes for partial differential equations with discontinuous coefficients, fast simulation of electromagnetic wave guiding, scattering and propagation in inhomogeneous media, and mathematical modeling of molecular surfaces in the implicit solvent theory.